Title	Trikoveramides A-C, cyclic depsipeptides from the marine cyanobacterium Symploca hydnoides
Author(s)	Ma Yadanar Phyo, Nursheena Parveen Katermeran, Jun Xian Goh and Lik Tong Tan

The final publication is available at: https://doi.org/10.1016/j.phytochem.2021.112879

Trikoveramides A-C, cyclic depsipeptides from the marine cyanobacterium *Symploca hydnoides*

Ma Yadanar Phyo, Nursheena Parveen Katermeran, Jun Xian Goh, Lik Tong Tan*

Natural Sciences and Science Education, National Institute of Education, Nanyang Technological University, 1 Nanyang Walk, Singapore 637616, Singapore

*Corresponding author: Tel: +65 6790 3842; Fax: +65 6896 9414

E-mail address: liktong.tan@nie.edu.sg (L.T. Tan)

ABSTRACT

Trikoveramides A – C, members of the kulolide superfamily of cyclic depsipeptides, were isolated from the marine cyanobacterium, *Symploca hydnoides*, collected from Bintan Island, Indonesia. Their planar structures were elucidated by a combination of NMR spectroscopy and HRMS spectral data. The absolute configurations of the amino acid and phenyllactic acid units were confirmed by Marfey's and chiral HPLC analyses, respectively, while the relative stereochemistry of the 3-hydroxy-2-methyl-7-octynoic acid (Hmoya) unit in trikoveramide A was elucidated by the application of the *J*-based configuration analysis and NOE correlations. The cytotoxic activity of the trikoveramides were evaluated against MOLT-4 human leukaemia cells and gave IC_{50} values of 9.3 μM, 35.6 μM and 48.8 μM for trikoveramide B, trikoveramide C and trikoveramide A, respectively. In addition, trikoveramides A – C showed weak to moderate inhibition in the quorum sensing inhibitory assay based on the *Pseudomonas aeruginosa lasB-gfp* and *rhlA-gfp* bioreporter strains.

Keywords: *Symploca hydnoides*; Microcoleaceae; Kulolide superfamily; Cyclic depsipeptides; Trikoveramides

1. Introduction

Filamentous marine cyanobacteria are prolific sources of chemically diverse and biologically active classes of specialised metabolites with potential pharmaceutical applications, including apratoxin A, gallinamide A, coibamide A, largazole, santacruzamate A and the recently discovered gatorbulin-1 (Linington et al., 2009; Pavlik et al., 2013; Al-Awadhi et al., 2020; Tranter et al., 2020; Kazemi et al., 2021; Matthew et al., 2021). *Lyngbya*, *Moorea*, *Symploca* and *Oscillatoria* are the major genera where at least 550 specialised metabolites have been isolated and identified (Nunnery et al., 2010; Tan and Phyo, 2020). These natural products belong mostly to the hybrid polyketide-peptide structural class and have been isolated mainly from the genus *Lyngbya*/*Moorea* (Tan, 2007; Tan, 2010). In addition, marine cyanobacterial specialised metabolites are characterised by their distinct *N*-methylation, α- and β-hydroxy acids and fatty acyl units.

The kulolide superfamily of cyclic depsipeptides is one such hybrid polyketide-peptide structural class. Since the first discovery of kulolide by Scheuer and co-workers (Reese et al., 1996) from the cephalaspidean mollusk, *Philinopsis speciosa*, a variety of kulolide-related molecules have been reported from filamentous marine cyanobacteria, including *Lyngbya majuscula* (*Moorea producens*), *Moorea* sp., *Symploca* cf. *hydnoides*, *Oscillatoria* sp. and *Rivularia* sp. (Boudreau et al., 2012). Members of the kulolide superfamily are characterized by the presence of either a 2,2-dimethyl-3-hydroxy-7-octynoic acid (Dhoya) or a 3-hydroxy-2-methyl-7-octynoic acid (Hmoya) moiety within seven (e.g. pitipeptolides, dudawalamides and viequeamides) or six (e.g. antanapeptins, trungapeptins, hantupeptins and veraguamides) residues containing cyclic depsipeptides, respectively. Reduced equivalents of Dhoya- and Hmoya-containing compounds, such as Dhoea (2,2-dimethyl-3-hydroxy-7-octenoic acid)/Dhoaa (2,2-dimethyl-3-hydroxy-7-octanoic acid) as well as Homea (3-hydroxy-2-methyl-7-octenoic acid)/Homaa (3-hydroxy-2-methyl-7-octanoic acid), respectively, have also been reported. In addition, a unique bromine containing Hmoya unit was found in veraguamides A and B (Mevers et al., 2011; Salvador et al., 2011). With the exception of hantupeptin A, veraguamide A and viequeamide A, a majority of the reported compounds showed moderate cytotoxic and antiparasitic activities.

We have previously isolated trikoramide A, a cytotoxic prenylated cyanobactin from Bintan (Phyo et al., 2019). Examination of the other polar fractions by ^{1}H NMR indicated the presence of a polyketide-polypeptide structural class. Further purification of this polar

fraction using RP-HPLC led to the isolation of three hitherto undescribed cyclic hexadepsipeptides, trikoveramides A (**1**) – C (**3**).

2. Results and discussion

2.1. Structural elucidation

Samples of *Symploca hydnoides* Kützing ex Gomont 1892 (Microcoleaceae) were collected by hand from the intertidal regions at Trikora beach, Bintan Island, Indonesia (Latitude 1° 9′ 16.8762″/Longitude 104° 34′ 42.0312″). The cyanobacterial samples were extracted exhaustively with CH_2Cl_2:MeOH (2:1) and the pooled extracts subjected to normal phase Si vacuum liquid chromatography (NP-VLC) to obtain eight fractions. The VLC-fraction, eluted with 100% EtOAc, was subjected to fractionation by reversed-phase solid phase extraction (RP-SPE), followed by a series of preparative reversed-phase HPLC purifications to afford trikoveramides A (**1**) – C (**3**) as white amorphous solids (Fig. 1). The three compounds exhibited very similar ^{1}H and ^{13}C NMR spectral data but had mass differences of 2 amu between trikoveramides A (**1**) and B (**2**) as well as between trikoveramides B (**2**) and C (**3**) (Supplementary Figs. S1, S2, S9, S10, S14 and S15).

Trikoveramide A (**1**) gave a $[M+H]^+$ protonated peak at *m/z* 723.4340, which was consistent with the molecular formula $C_{40}H_{58}N_4O_8$ requiring 14 degrees of unsaturation (Supplementary Fig. S19). The ^{1}H NMR spectrum of **1** portrayed characteristic peptide resonances for secondary amide proton (δ_H 6.30), two tertiary amide *N*-CH_3 (δ_H 3.06, δ_H 2.62) and various α-protons (δ_H 3.90-5.00) (Supplementary Fig. S1). Detailed analysis of the 1D and 2D NMR data allowed the assembly of six partial structures (Table 1). A combination of 2D NMR experiments, including HSQC, HMBC and COSY, revealed the presence of four standard amino acid residues, including one proline (Pro), one valine (Val) and two *N*-methylvaline (*N*-Me-Val) as well as two hydroxy acid units (Supplementary Figs. S3 to S7). The presence of a low-field α-proton (δ_H 5.47) of the hydroxy acid unit and its COSY correlations to diastereotopic CH_2 protons at δ_H 3.16/δ_H 2.92, coupled with HMBC correlations of the latter to aromatic carbons at δ_C 136.2 and 129.3, established the presence of a 3-phenyllactic acid (Pla) residue. The second β-hydroxy acid unit was constructed based on 1D and 2D NMR data. Analysis of the ^{13}C NMR showed a quaternary carbon resonance at δ_C 83.6 and a methine carbon signal at δ_C 68.9 bonded to a high field proton at δ_H 1.95 which was characteristic for a terminal alkyne functional group. Assembly of the remaining signals, namely δ_C/δ_H 77.2/4.89, 42.2/3.23, 27.6/1.65 and 2.08, 25.2/1.45 and 1.64, 18.0/2.21,

14.6/1.30, by 2D NMR identified this unit as 3-hydroxy-2-methyl-7-octynoic acid (Hmoya). Four key HMBC correlations between H-3 (Hmoya)/C-1 (*N*-Me-Val-1), *N*CH_3 (*N*-Me-Val-1)/C1 (Pro), H-2 (Pla)/C-1 (*N*-Me-Val-2), *N*CH_3 (*N*-Me-Val-2)/C-1 (Val) allowed the connection of the partial structures to provide the Hmoya-*N*Me-Val-1-Pro and Pla-*N*Me-Val-2-Val sequences. HMBC correlations between C-1 of Pla and H-5b of Pro and a further ROESY correlation between H-2 of Pla and H-2/H-5b of Pro allowed the assembly of the two sequences into Hmoya-*N*-Me-Val-1-Pro-Pla-*N*-Me-Val-2-Val. Additional HMBC correlations between the H-2 of Val and the C-1 of the Hmoya moiety completed the cyclic planar structure of trikoveramide A having 14 degrees of unsaturation (Fig. 1). The collision induced dissociation (CID) MS/MS fragmentation pattern observed under positive electrospray ionization (ESI) mode further confirmed the sequence derived from the NMR experiments (Fig. 2). For instance, compound **1** underwent ring-opening to form a linear acylium ion with *N*-Me-Val at the C terminus. Sequential C-terminal cleavage resulted in a series of b-ions as observed in the MS/MS fragmentation spectrum of **1** (Supplementary Fig. S19).

The absolute stereochemical configuration of the amino acid units in trikoveramide A (**1**) was determined by Marfey's analysis (Marfey, 1984). Acid hydrolysis of **1** and subsequent derivatization with Marfey's reagent revealed the L-configuration of Val, *N*-Me-Val and Pro residues. The absolute stereochemistry of the Pla unit was determined as D form by chiral HPLC analysis. *J*-based configuration analysis, based on HSQC-HECADE NMR experiments and NOE correlations, were applied to determine the relative stereochemistry of C-2 and C-3 of the Hmoya unit in **1** (Koźmiński and Nanz, 1997; Matsumori et al., 1999). A NOE correlation was observed between the H-2 and H-3 of the Hmoya unit and a small ^3J_H coupling constant value of 2.20 Hz was calculated between the H-2 and H-3 (Supplementary Fig. S5). These combined data established a syn configuration between the H-2 and H-3 of the Hmoya unit. In the HSQC-HECADE spectrum, a small heteronuclear coupling of $^3J_{H3\text{-}C9}$ = 2.44 Hz was consistent with a gauche arrangement of H-3 and CH_3-9 (Supplementary Fig S8). Furthermore, a large $^2J_{H2\text{-}C3}$ = -5.26 Hz also implied a gauche arrangement between the H-2 and the oxygen of the ester linked moiety on C-3 (Fig. 3). Taken together, a relative stereochemistry of 2*S** and 3*R** was established for C-2 and C-3, respectively, in the Hmoya unit. This was consistent with the configurations of the C-2 and C-3 of the Hmoya unit in veraguamide F. A direct comparison of the 1D NMR spectral data of veraguamide F (Salvador et al., 2011) and compound **1** further indicated that these two molecules should

have similar configurations at C-2 and C-3 of the Hmoya moiety. Due to insufficient quantity of the molecule, the absolute stereochemistry of the Hmoya unit was not established via chemical manipulations, which would entail methanolysis and isolation of the Hmoya-containing fragment for Mosher's analysis.

Trikoveramide B (**2**) gave a $[M+H]^+$ protonated molecule at *m/z* 725.4485 by HR-ESI-OrbitrapMS, two mass units higher than that of trikoveramide A (**1**), giving a molecular formula of $C_{40}H_{60}N_4O_8$ (Supplementary Fig. S20). Analysis of their 1D NMR spectral data showed that compounds **2** and **1** have nearly identical ^1H and ^{13}C NMR chemical shifts, demonstrating that they are structurally related (Supplementary Figs. S9 and S10). The main differences were in the Hmoya unit where in trikoveramide B (**2**), the acetylene carbon signals of **1** were replaced by new methine (δ_C 138.1, δ_H 5.75) and methylene signals (δ_C 115.5, δ_H 4.99 and 4.95), which were characteristic of a monosubstituted olefin functional group. These chemical shifts suggest the partial reduction of the terminal triple bond in **1** to a double bond in **2**. This is confirmed from the analysis of 2D NMR spectral data on the presence of a 3-hydroxy-2-methyloct-7-enoic-acid (Hmoea) unit in **2** (Fig. 1 and Supplementary Figs. S11 – S13).

A high resolution MS spectrum of trikoveramide C (**3**) established its molecular formula as $C_{40}H_{62}N_4O_8$ with $[M+H]^+$ peak at *m/z* 727.4651, which is 2 mass units more than that of trikoveramide B (**2**) giving a molecular formula of $C_{40}H_{62}N_4O_8$ (Supplementary Fig. S21). The ^1H and ^{13}C NMR chemical shifts of **3** were also nearly identical to those for **1** and **2** but a closer examination revealed differences in the chemical shifts for only the β-hydroxy unit (Supplementary Figs. S14 and S15). The ^1H NMR signals in the olefinic region at δ_H 5.75, 4.99 and 4.95 in **2** was replaced by the high field methylene signals at δ_H 1.31 and 0.87 in **3**. These corresponded to high field carbon resonances at δ_C 22.5 and 13.9, respectively, in the ^{13}C NMR spectrum implying that the terminal double bond of Hmoea in **2** has been reduced to single bond in **3** resulting in a 3-hydroxy-2-methyloct-7-anoic-acid (Hmoaa) unit instead (Fig. 1). Since the ^1H and ^{13}C NMR data, as well as the optical rotations for compounds **2** and **3**, were almost identical with those of **1**, stereochemical analysis was not performed on **2** and **3** with the assumption that they possessed the same absolute and relative configurations as well as sharing a common biosynthetic pathway.

The trikoveramides belong to the kulolide superfamily where the sequence of the different residues are highly conserved and are derived from a mix of the NRPS-PKS

biosynthetic pathway (Boudreau et al., 2012). Trikoveramide A displayed similar NMR chemical shifts to veraguamide F (Salvador et al., 2011) and they essentially have the same sequence of peptides bearing the same sequence of amino acids. The only difference is in the stereochemistry where in veraguamide F, the absolute configuration of 3-phenyllactic acid was reported as 2*S*-Pla, whereas in trikoveramide A (**1**) the configuration is 2*R*-Pla.

*2.2. Biological activity of trikoveramides A (**1**) – C(**3**)*

Trikoveramides A (**1**) - C (**3**) were screened for their biological activities in the *in vitro* cytotoxicity assay based on the MOLT-4 human leukemia cell line. Trikoveramide B (**2**) was found to be the most cytotoxic of the three compounds, giving an IC_{50} value of 9.32 μM. Trikoveramides A (**1**) and C (**3**) displayed weak cytotoxicity with IC_{50} values of 48.8 μM and 35.6 μM, respectively (Fig. 4). This seems to suggest that the β-hydroxy acid group plays a significant role in the cytotoxicity of the molecules. Compound **2** having the Hmoea moiety containing the vinylic protons enhanced the cytotoxic activity in the MOLT-4 leukemia cell line assay by at least four times as compared to the Hmoya and the Hmoaa units in **1** and **3**, respectively. Similarly, hantupeptin B, containing the Hmoea unit, was also found to be the most potent among the three analogues in the *in vitro* cytotoxicity assays against MOLT-4 and MCF-7 cancer cell lines with IC_{50} values of 0.2 μM and 0.3 μM, respectively (Tripathi et al., 2010). It is interesting that subtle amino acid/hydroxy units change of the *N*-Me-Ile, *S*-Pla and 2*R*,3*S*-Hmoea units in hantupeptin B to *N*-Me-Val, *R*-Pla and 2*S**,3*S**-Hmoea moieties in trikoveramide B (**2**) decreased the cytotoxic activity in the MOLT-4 cancer cell line by ten folds in the latter molecule.

Compounds **1** – **3** also exhibited weak to moderate activity in the quorum sensing inhibitory assay based on the *Pseudomonas aeruginosa lasB-gfp* as well as the *rhlA-gfp* bioreporter strains. Tested at 100 μM, trikoveramide C showed the highest activity with 45% reduction in fluorescence, while **1** and **2** exhibited 8% and 26% inhibition, respectively, based on the *P. aeruginosa lasB-gfp* biosensor strain. The inhibitory activity decreases with the increase in the unsaturation of the bonds from Hmoaa to Hmoya. Little or no reduction in fluorescence was observed when compounds were tested using the *P. aeruginosa rhlA-gfp* bioreporter strain. However, trikoveramides did not show dose dependent activity when tested at various concentrations.

The discovery of the trikoveramides from *S. hydnoides* in this study adds to the growing class of the kulolide superfamily, under the Hmoya subgroup consisting of six residues cyclic

depsipeptides. These molecules include the kulomo'opunalides, tiahuramides, hantupeptins, veraguamides, antanapeptins and trungapeptins (Nakao et al., 1998; Nogle et al., 2002; Bunyajetpong et al., 2006; Tripathi et al., 2009; Tripathi et al., 2010; Mevers et al., 2011; Salvador et al., 2011; Levert et al., 2018). It is intriguing that although the structures within the kulolide superfamily (Hmoya subgroup) are highly conserved, they display varying biological activities. For instance, tiahuramides A – C were reported to have antibacterial and cytotoxic activities as well as inhibiting the first cell division of sea urchin fertilised eggs (Levert et al., 2018). Trungapeptin A exhibited brine shrimp toxicity but was not cytotoxic on KB and LoVo cells when tested at 10 µg/mL (Bunyajetpong et al., 2006). Veraguamides A – F showed moderate to weak cytotoxicity against HT29 colorectal adenocarcinoma and HeLa cervical carcinoma cell lines (Salvador et al., 2011). On the other hand, antanapeptins A – D did not exhibit any biological activities when tested in a series of biological assays, including the brine shrimp toxicity, sodium channel modulation and antimicrobial bioassays (Nogle and Gerwick, 2002).

3. Conclusions

Three hitherto undescribed compounds, trikoveramides A (**1**) – C (**3**) have been isolated from the marine cyanobacterium *S. hydnoides* collected from Bintan Island, Indonesia. Trikoveramides exhibited moderate to weak cytotoxicity against the MOLT-4 human leukemia cancer cell line, with trikoveramide B having the highest activity. In addition, these compounds exhibited weak to moderate quorum sensing inhibitory activity based on the *P. aeruginosa lasB-gfp* biosensor strain. Due to the wide occurrence of the kulolide superfamily related compounds reported mainly from various pan-tropical marine filamentous cyanobacterial species, it is possible that these molecules have an ancient evolutionary origin within the cyanobacteria as well as possessing essential ecological functions.

4. Experimental

4.1. General experimental procedures

Optical rotations were measured on an Anton Paar Polarimeter while UV and IR spectral readings were measured on a PerkinElmer UV-Visible spectrophotometer and a PerkinElmer spectrum 100 FT-IR spectrophotometer, respectively. All NMR spectra were recorded in $CDCl_3$ on a 400 MHz Bruker NMR Spectrometer (400.13 MHz ^{1}H, 100.61 MHz ^{13}C) using residual solvent signals as internal references (referenced to residual CDCl3 observed at δ_H

7.24 or δ_C 77.0) with chemical shifts given in ppm downfield from TMS. Isolation and purification of the trikoveramides were conducted on a Shimadzu LC-8A preparative LC coupled to a Shimadzu SPD-M10A VP diode array detector HPLC. All chemicals used for Marfey's analysis were purchased from Sigma-Aldrich. Hexanes, dichloromethane (CH_2Cl_2), ethyl acetate (EtOAc) and methanol (MeOH) were purchased from Fisher Chemical, USA and were of HPLC grade. High resolution MS data and MS/MS data were acquired on a Q Exactive™ Plus Hybrid Quadrupole-Orbitrap Mass Spectrometer (Thermo Fisher Scientific, USA) equipped with a heated electrospray ionization (H-ESI) probe.

4.2. Sample collection

Marine cyanobacterial samples, with cell morphology resembling that of the genus *Symploca hydnoides* Kützing ex Gomont 1892 (Microcoleaceae), were collected in April 2018 by hand from the intertidal shores of Trikora beach, Bintan Island (Latitude 1º 9′ 16.8762″/Longitude 104º 34′ 42.0312″) and subsequently stored in 70% EtOH at -20 ºC before workup at NIE. The voucher specimen, TLT/Tri/22Apr2018/001, is deposited at Natural Sciences and Science Education, National Institute of Education, Singapore.

4.3. Extraction and isolation of compounds

Microbial samples (ca. 2.0 L, wet weight) were thawed and extracted exhaustively with 2:1 CH_2Cl_2/MeOH. After the solvent was evaporated *in vacuo*, 1.19 g of a crude organic extract was obtained. The extract was then extracted using normal phase Si gel column chromatography using stepwise gradient with increasing polarity of 100% hexanes, hexanes/ETOAc (9:1, *v/v*), hexanes/EtOAc (4:1, *v/v*), hexanes/EtOAc (3:2, *v/v*), hexanes/EtOAc (2:3, *v/v*), hexanes/EtOAc (1:4, *v/v*), 100% EtOAc and EtOAc/MeOH (9:1, *v/v*). Fraction 7, eluted with 100% EtOAc, was subjected to solid-phase fractionation on a Sep-Pak C_{18} cartridge (Phenomenex, Torrance, CA, USA) using 100% MeOH to remove pigments. The resulting filtrate was further subjected to semi-preparative RP-HPLC separation (Phenomenex Luna 5µm Phenyl-Hexyl, 250 × 10mm, 85% MeOH/H_2O in 40 min at 3.0 mL/min, detected at 210 nm, 230 nm and 290 nm) to yield semi-pure trikoveramides A-C. A final purification was achieved using semi-preparative RP-HPLC (Phenomenex Kinetex 5 µm C_{18}, 250 × 4.6 mm, 85% MeOH/H_2O) to yield pure trikoveramides A (**1**) - C (**3**) (**1**, 1.0 mg, t_R = 18.9 min, **2**, 0.7 mg, t_R = 25.1 min, **3**, 0.8 mg, t_R = 29.2 min).

4.4. Compound characterisation data

Trikoveramide A (**1**): white amorphous solid; $[\alpha]_D^{20}$ -41 (c 0.15, MeOH); IR (Nujol) ν_{max} 3451, 3300, 2960, 2869, 1735, 1650, 1493 cm^{-1}; UV (MeOH) λ_{max} (log ε) 203 nm; ^1H and ^{13}C NMR data ($CDCl_3$, 400.13 and 100.61 MHz, respectively), see Table 1 and Supplementary Data; HR-ESI-OrbitrapMS *m/z* 723.4340 $[M+H]^+$ (calcd for $C_{40}H_{59}N_4O_8$, 723.4327).

Trikoveramide B (**2**): white amorphous solid; $[\alpha]_D^{20}$ -42.3 (c 0.12, MeOH); IR (Nujol) ν_{max} 3450, 3300, 2965, 2869, 1735, 1650, 1491 cm^{-1}; UV (MeOH) λ_{max} (log ε) 203 nm; ^1H and ^{13}C NMR data ($CDCl_3$, 400.13 and 100.61 MHz, respectively), see Table 1 and Supplementary Data; HR-ESI-OrbitrapMS *m/z* 725.4485 $[M+H]^+$ (calcd for $C_{40}H_{61}N_4O_8$, 725.4484).

Trikoveramide C (**3**): white amorphous solid; $[\alpha]_D^{20}$ -41.4 (c 0.13, MeOH); IR (Nujol) ν_{max} 3452, 3305, 2965, 2869, 1735, 1652, 1495 cm^{-1}; UV (MeOH) λ_{max} (log ε) 203 nm; ^1H and ^{13}C NMR data ($CDCl_3$, 400.13 and 100.61 MHz, respectively), see Table 1 and Supplementary Data; HR-ESI-OrbitrapMS *m/z* 727.4651 $[M+H]^+$ (calcd for $C_{40}H_{63}N_4O_8$, 727.4640).

*4.5. Marfey's analysis of amino acids in **1***

Acid hydrolysis of trikoveramide A (**1**, 200 μg) was achieved in 0.5 mL of 6N HCl placed in a sealed reaction vial purged with N_2 gas at 115 ºC for 18 h. Trace HCl was then removed *in vacuo* and the resulting hydrolysate was redissolved in 0.1 mL of H_2O. A 1% solution of L-FDAA (1-fluoro-2,4-dinitrophenyl-5-L-alaninamide) (100 μL) in acetone and 1N $NaHCO_3$ (20 μL) was added to the aqueous hydrolysate and the mixture subsequently was heated at 50 ºC for 3 h. Once the resulting mixture was cooled to rt, it was sequentially quenched with 2N HCl (50 μL), then dried under vacuum and resuspended in 1:1 H_2O/CH_3CN (*v/v*) for RP-HPLC analysis. Each HPLC analysis was carried out using a Shimadzu Shimpak C_{18} column (250 × 4.6 mm, 2.6 μm) isocratically eluted with CH_3CN/0.05 M trifluoroacetic acid, (2:3, *v/v*) at a 1.0 mL/min flow rate. The retention times t_{RL}/t_{RD} in min of the L-DAA monoderivatized standards were: Pro (6.96/7.40), Val (10.7/14.7), *N*-Me-Val (14.1/17.2). The derivatized hydrolysate peaks of **1** gave retention times at 6.91 min, 10.6 min and 14.1 min, which corresponded to L-Pro, L-Val and L-*N*-Me-Val, respectively.

*4.6. Absolute stereochemistry of the 3-phenyllactic acid in **1***

Trikoveramide A (**1**, 100 μg) was hydrolysed in 6N HCl at 105 ºC for 15 h. The hydrosylate was concentrated to dryness and analysed by chiral HPLC column (Phenomenex

Chirex® 3126 (D)-penicillamine, 50 x 4.6 mm), flow rate 1.0 mL/min, detection at 254 nm, with 1 mM $CuSO_4$/IPA (85:15). Phenyllactic acid in hydrosylate eluted at t_R = 38.1 min corresponding to the retention time of an authentic standard of D-3-phenyllactic acid and therefore indicating an *R* configuration (t_R of L-3-phenyllactic acid = 32.8 min).

4.7. MOLT-4 human leukemia cell line assay

Assessment of the cytotoxicity of compounds **1** - **3** was carried out using the MTT bioassay based on the MOLT-4 (T lymphoblast; acute lymphoblastic leukemia), cancer cell line over a 3-day procedure. On the first day, **1** was prepared in a 96-well microtiter plate at 10 mM stock concentration dissolved in 100% DMSO, conducted in triplicate. The mixtures were then added with RPMI media, supplemented with fetal calf serum; and serial diluted to give concentrations of 125, 50, 20, 8 and 3.2 µM. To each of the concentration, 10 µL of the diluted compound **1** was added with 70 µL of the cancer cells. The plate was incubated for 24 h in a 37 °C, 5% CO_2 incubator. On day 2, 20 µL of MTT solution were added to each of the wells and incubated for 3 h. Another 100 µL of lysing buffer was added to each well thereafter and incubated overnight. On day 3, the microtiter plate was measured at OD570 nm and the results were tabulated.

4.8. Quorum sensing inhibitory assay

The anti-quorum sensing bioassay was carried out using *Pseudomonas aeruginosa* reporter strains (Yang et al., 2007). Compounds **1** - **3** were prepared in a 96-well microtiter plate at 10 mM stock concentration dissolved in 100% DMSO, conducted in triplicate. Compounds **1** - **3** were then mixed with ABTGC medium; and serial diluted to give a concentration of 20 µM in the first dilution factor (with 0.2% of DMSO). A total of seven dilution factors, down to 0.3125 µM were done. An overnight culture of PAO1-*lasB-gfp* strain (Hentzer et al., 2002), grown in lysogeny broth at 37 °C, 200 rpm, was diluted in ABTGC medium to an optical density of 0.02 at OD_{600} which correspond to 2.5×10^7 CFU/mL. An equal amount of the bacterial suspension was added to reach a final test concentration of 10, 5, 2.5, 1.25, 0.625, 0.3125, and 0.1563 µM. A DMSO control, media control and culture control were used and the microtiter plates were incubated at 37 °C in a Tecan Infinite 200 Pro plate reader to measure the cell density (OD_{600}) and green fluorescence protein fluorescence (excitation at 483 nm, emission at 535 nm) with 15 min

intervals for up to 16 h. Similar procedure was carried out using the PAO1-*rhlA-gfp* biosensor strain.

Declaration of competing interest

The authors declare that they have no known competing financial interests or personal relationships that could have appeared to influence the work reflected in this paper.

Acknowledgements

The facilities and equipment support were provided partially by the National Institute of Education, Singapore. This research is supported by the National Research Foundation, Prime Minister's Office, Singapore under its Marine Science Research and Development Programme (Award Nos. MSRDP-P15 and MSRDP-P34), NIE AcRF grant (RI 2/20/TLT) as well as the Nanyang Technological University Research Scholarship (Reg No. 200604393R).

Appendix A. Supplementary data

Supplementary data related to this article can be found online at https://XXX

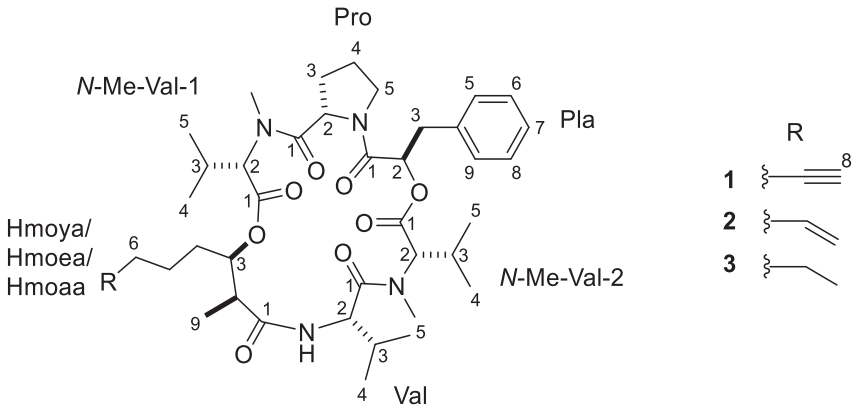

Fig. 1. Structures of trikoveramides A (**1**) – C (**3**).

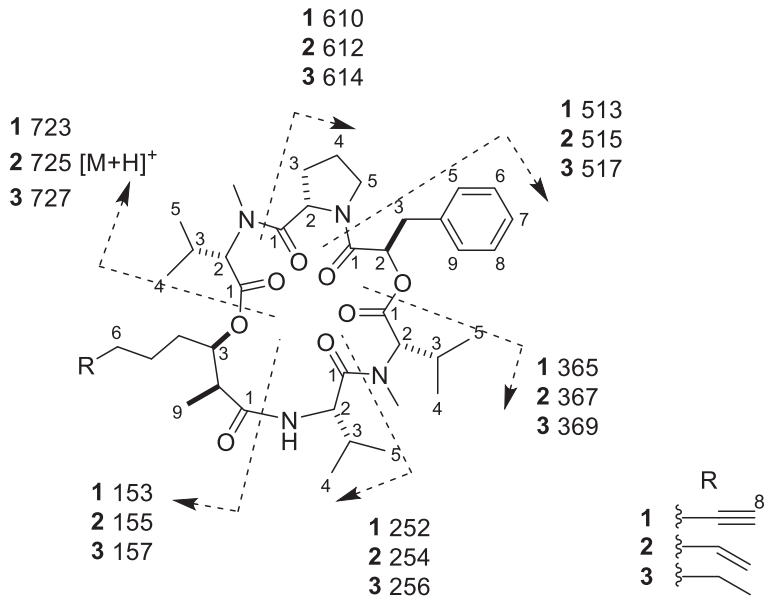

Fig. 2. Mass spectrometric fragmentation of trikoveramides A (**1**) – C (**3**).

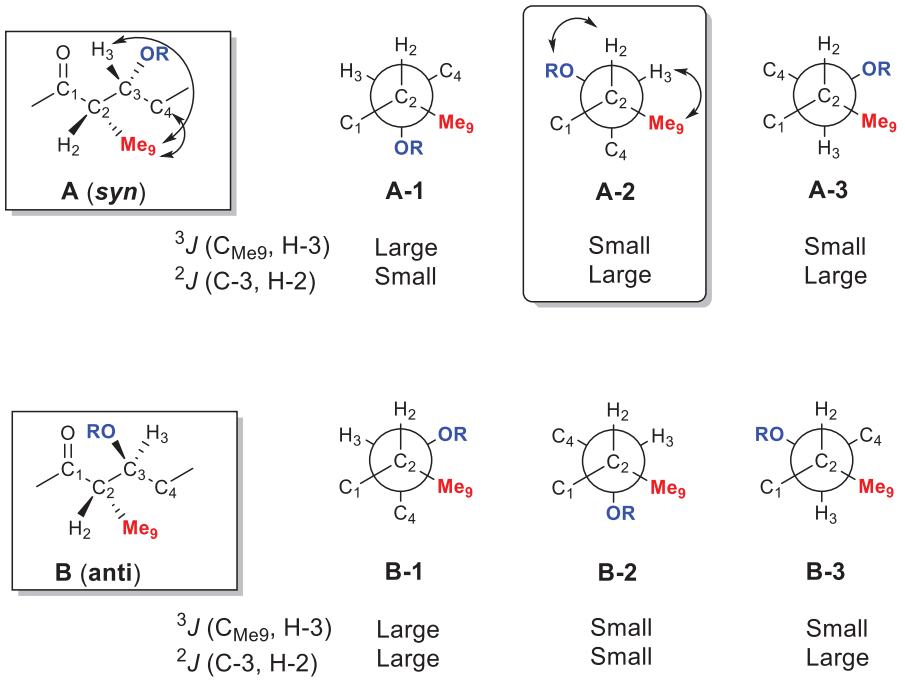

Fig. 3. Newman projections for C-2/C-3 of the Hmoya unit in trikoveramide A (**1**). Labels below projections denote predicted size of the ^3J(C_{Me9}, H-3) and ^2J(C-3,H-2) coupling constants. Predicted values highlighted by a box are consistent with observed coupling constant values. Double-headed arrows indicate NOE correlations.

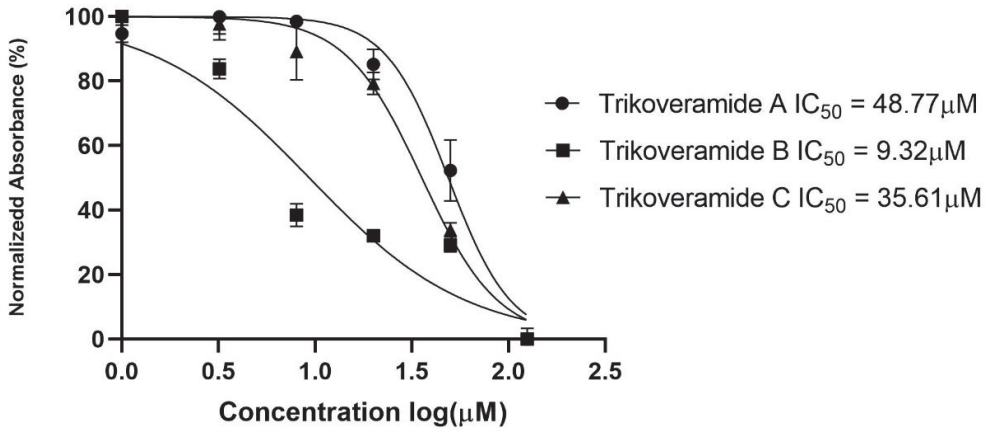

Fig. 4. Graph showing log concentration of trikoveramides (μM) against normalised absorbance (%) for the MTT assay performed on MOLT-4 human leukemia cell line.

Table 1

^{1}H NMR (400 MHz) and ^{13}C NMR (100 MHz) data of trikoveramides A (**1**) - C (**3**) in $CDCl_3$.

Unit	Position	Trikoveramide A (**1**)		Trikoveramide B (**2**)		Trikoveramide C (**3**)	
		δ_C, type	δ_H (*J* in Hz)	δ_C, type	δ_H (*J* in Hz)	δ_C, type	δ_H (*J* in Hz)
Hmoya/	1	170.8, C		170.8, C		170.7, C	
Hmoea/	2	42.2, CH	3.23, qd (7.4, 2.2)	42.3, CH	3.22, m	42.2, CH	3.21, m
Hmoaa	3	77.2, CH	4.89, dt (10.7, 2.2)	76.9, CH	4.87, dt (10.7, 2.2)	77.2, CH	4.88, dt (10.7, 2.2)
	4a	27.6, CH_2	2.08, m	27.9, CH_2	1.97, m	29.7, CH_2	1.24, m
	4b		1.65, m		1.50, m		1.54, m
	5a	25.2, CH_2	1.64, m	25.6, CH_2	1.49, m	26.1, CH_2	1.41, m
	5b		1.45, m		1.29, m		1.21, m
	6	18.0, CH_2	2.21, m	33.2, CH_2	2.07, m	31.4, CH_2	1.90, m 1.29, m
	7	83.6, C		138.1, CH	5.75, m	22.5, CH_2	1.31, m
	8	68.9, CH	1.95, t (2.7)	115.5, CH_2	4.99, m 4.95, m	13.9, CH_3	0.87, t (6.7)
	9	14.6, CH_3	1.30, d (7.4)	14.5, CH_3	1.27, d (7.7)	14.1, CH_3	1.26, d (7.7)
N-Me-	1	171.0, C		171.1, C		171.2, C	
Val-1	2	65.3, CH	3.95, d (10.8)	65.4, CH	3.95, d (10.6)	65.3, CH	3.95, d (10.6)
	3	28.3, CH	2.93, m	28.3, CH	2.94, m	28.4, CH	2.93, m
	4	19.7, CH_3	1.01, d (6.5)	19.6, CH_3	1.02, d (6.8)	19.5, CH_3	1.01, d (6.5)
	5	19.8, CH_3	1.02, d (6.5)	19.7, CH_3	1.03, d (6.6)	19.7, CH_3	1.03, d (6.5)
	N-Me	28.7, CH_3	3.06, s	28.9, CH_3	3.06, s	28.7, CH_3	3.06, s
Pro	1	172.3, C		172.4, C		172.4, C	
	2	57.2, CH	4.97, m	57.2, CH	4.98, m	57.2, CH	4.98, m

Unit	Position	Trikoveramide A (**1**)		Trikoveramide B (**2**)		Trikoveramide C (**3**)	
		δ_C, type	δ_H (*J* in Hz)	δ_C, type	δ_H (*J* in Hz)	δ_C, type	δ_H (*J* in Hz)
	3a	29.1, CH_2	2.27, m	29.2, CH_2	2.28, m	29.1, CH_2	2.28, m
	3b		1.83, m		1.83, m		1.82, m
	4a	25.1, CH_2	2.08, m	25.0, CH_2	2.07, m	25.1, CH_2	2.07, m
	4b		1.98, m		1.96, m		1.98, m
	5a	47.1, CH_2	3.59, m	47.0, CH_2	3.58, m	47.1, CH_2	3.59, m
	5b		3.62, m		3.62, m		3.63, m
Pla	1	165.5, C		165.4, C		165.5, C	
	2	72.9, CH	5.47, dd (9.8, 4.2)	72.8, CH	5.48, dd (10.6, 4.1)	72.9, CH	5.48, dd (10.7, 4.1)
	3	36.6, CH_2	3.16, m 2.92, m	36.6, CH_2	3.18, m 2.91, m	36.7, CH_2	3.15, m 2.91, m
	4	136.2, C		136.2, C		136.3, C	
	5/9	129.3, CH	7.17, m	129.3, CH	7.18, m	129.4, CH	7.19, m
	6/8	128.5, CH	7.28, m	128.5, CH	7.27, m	128.5, CH	7.29, m
	7	126.8, CH	7.19, d (8.0)	126.7, CH	7.21, m	126.7, CH	7.22, m
N-Me-	1	169.0, C		168.9, C		168.9, C	
Val-2	2	65.9, CH	4.07, d (10.3)	65.8, CH	4.10, d (10.4)	65.9, CH	4.08, d (10.4)
	3	27.5, CH	2.09, m	27.4, CH	2.09, m	27.4, CH	2.07, m
	4	20.0, CH_3	0.94, d (6.5)	20.0, CH_3	0.92, d (6.5)	20.3, CH_3	0.94, d (6.5)
	5	19.9, CH_3	1.03, d (6.6)	19.8, CH_3	1.01, d (6.5)	19.9, CH_3	1.02, d (6.6)
	N-Me	29.2, CH_3	2.62, s	29.0, CH_3	2.60, s	29.1, CH_3	2.59, s
Val	1	173.5, C		173.5, C		173.4, C	
	2	52.8, CH	4.76, dd (8.9, 6.1)	52.7, CH	4.76, dd (8.7, 6.1)	52.7, CH	4.77, dd (8.9, 6.1)
	3	32.3, CH	1.97, m	32.3, CH	1.97, m	32.3, CH	1.97, m
	4	20.3, CH_3	0.91, d (6.5)	20.2, CH_3	0.94, d (6.8)	19.6, CH_3	0.92, d (6.5)

Unit	Position	Trikoveramide A (**1**)		Trikoveramide B (**2**)		Trikoveramide C (**3**)	
		δ_C, type	δ_H (*J* in Hz)	δ_C, type	δ_H (*J* in Hz)	δ_C, type	δ_H (*J* in Hz)
	5	17.6, CH_3	0.88, d (6.7)	17.7, CH_3	0.88, d (6.8)	17.6, CH_3	0.88, d (6.8)
	*N*H		6.30, d (8.6)		6.26, d (8.8)		6.26, d (8.8)

[a] HMBC correlations optimized for $^{2/3}J_{CH}$ = 8.0 Hz, are from protons stated to the indicated carbon.

References

Al-Awadhi, F.H., Salvador-Reyes, L.A., Elsadek, L.A., Ratnayake, R., Chen, Q.Y., Luesch, H., 2020. Largazole is a brain-penetrant class I HDAC inhibitor with extended applicability to glioblastoma and CNS diseases. ACS Chem. Neurosci. 11, 1937−1943. https://doi.org/10.1021/acschemneuro.0c00093.

Boudreau, P.D., Byrum, T., Liu, W.T., Dorrestein, P.C., Gerwick, W.H., 2012. Viequeamide A, a cytotoxic member of the kulolide superfamily of cyclic depsipeptides from a marine button cyanobacterium. J. Nat. Prod. 75, 1560−1570. https://doi.org/10.1021/np300321b.

Bunyajetpong, S., Yoshida, W.Y., Sitachitta, N., Kaya, K., 2006. Trungapeptins A−C, Cyclodepsipeptides from the marine cyanobacterium *Lyngbya majuscula*. J. Nat. Prod. 69, 1539−1542. https://doi.org/10.1021/np050485a.

Hentzer, M., Riedel, K., Rasmussen, T.B., Heydorn, A., Andersen, J.B., Parsek, M.R., Rice, S.A., Eberl, L., Molin, S., Høiby, N., Kjelleberg, S., Givskov, M., 2002. Inhibition of quorum sensing in *Pseudomonas aeruginosa* biofilm bacteria by a halogenated furanone compound. Microbiology 148, 87–102. https://doi.org/10.1099/00221287-148-1-87.

Kazemi, S., Kawaguchi, S., Badr, C.E., Mattos, D.R., Ruiz-Saenz, A., Serrill, J.D., Moasser, M.M., Dolan, B.P., Paavilainen, V.O., Oishi, S., McPhail, K.L., Ishmael, J.E., 2021. Targeting of HER/ErbB family proteins using broad spectrum Sec61 inhibitors coibamide A and apratoxin A. Biochem. Pharmacol. 183, 114317. https://doi.org/10.1016/j.bcp.2020.114317.

Koźmiński, W., Nanz, D., 1997. HECADE: HMQC- and HSQC-based 2D NMR experiments for accurate and sensitive determination of heteronuclear coupling constants from E.COSY-type cross peaks. J. Mag. Res. 124, 383−392. https://doi.org/10.1006/jmre.1996.1016.

Levert, A., Alvariño, R., Bornancin, L., Abou Mansour, E., Burja, A.M., Genevière, A.M., Bonnard, I., Alonso, E., Botana, L., Banaigs, B., 2018. Structures and activities of tiahuramides A–C, cyclic depsipeptides from a Tahitian collection of the marine cyanobacterium *Lyngbya majuscula*. J. Nat. Prod. 81, 1301−1310. https://doi.org/10.1021/acs.jnatprod.7b00751.

Linington, R.G., Clark, B.R., Trimble, E.E., Almanza, A., Ureña, L.D., Kyle, D.E., Gerwick, W.H., 2009. Antimalarial peptides from marine cyanobacteria: isolation and structural elucidation of gallinamide A. J. Nat. Prod. 72, 14−17. https://doi.org/10.1021/np8003529.

Marfey, P., 1984. Determination of D-amino acids. II. Use of a bifunctional reagent, 1, 5-difluoro-2, 4-dinitrobenzene. Carlsberg Res. Commun. 49, 591−596. https://doi.org//10.1007/BF02908688.

Matsumori, N., Kaneno, D., Murata, M., Nakamura, H., Tachibana, K., 1999. Stereochemical determination of acyclic structures based on carbon-proton spin-coupling constants. A method of configuration analysis for natural products. J. Org. Chem. 64, 866−876. https://doi.org/10.1021/jo981810k.

Matthew, S., Chen, Q.Y., Ratnayake, R., Fermaintt, C.S., Lucena-Agell, D., Bonato, F., Prota, A.E., Lim, S.T., Wang, X., Díaz, J.F., Risinger, A.L., Paul, V.J., Oliva, M.Á., Luesch, H., 2021. Gatorbulin-1, a distinct cyclodepsipeptide chemotype, targets a seventh tubulin pharmacological site. Proc. Natl. Acad. Sci. USA 118, e2021847118. https://doi.org/10.1073/pnas.2021847118.

Mevers, E., Liu, W.T., Engene, N., Mohimani, H., Byrum, T., Pevzner, P.A., Dorrestein, P.C., Spadafora, C., Gerwick, W.H., 2011. Cytotoxic veraguamides, alkynyl bromide-containing cyclic depsipeptides from the marine cyanobacterium cf. *Oscillatoria margaritifera*. J. Nat. Prod. 74, 928−936. https://doi.org/10.1021/np200077f.

Nakao, Y., Yoshida, W.Y., Szabo, C.M., Baker, B.J., Scheuer, P.J., 1998. More peptides and other diverse constituents of the marine mollusk *Philinopsis speciosa*. J. Org. Chem. 63, 3272–3280. https://doi.org/10.1021/jo9719867.

Nogle, L.M., Gerwick, W.H., 2002. Isolation of four new cyclic depsipeptides, antanapeptins A−D, and dolastatin 16 from a Madagascan collection of *Lyngbya majuscula*. J. Nat. Prod. 65, 21−24. https://doi.org/10.1021/np010348n.

Nunnery, J.K., Mevers, E., Gerwick, W.H., 2010. Biologically active secondary metabolites from marine cyanobacteria. Curr. Opin. Biotechnol. 21, 787−793. https://doi.org/10.1016/j.copbio.2010.09.019.

Pavlik, C.M., Wong, C.Y., Ononye, S., Lopez, D.D., Engene, N., McPhail, K.L., Gerwick, W.H., Balunas, M.J., 2013. Santacruzamate A, a potent and selective histone deacetylase

inhibitor from the Panamanian marine cyanobacterium cf. *Symploca* sp. J. Nat. Prod. 76, 2026−2033. https://doi.org/10.1021/np400198r.

Phyo, M.Y., Ding, C.Y.G., Goh, H.C., Goh, J.X., Ong, J.F.M., Chan, S.H., Yung, P.Y.M., Candra, H., Tan, L.T., 2019. Trikoramide A, a prenylated cyanobactin from the marine cyanobacterium *Symploca hydnoides*. J. Nat. Prod. 82, 3482−3488. https://doi.org/10.1021/acs.jnatprod.9b00675.

Reese, M.T., Gulavita, N.K., Nakao, Y., Hamann, M.T., Yoshida, W.Y., Coval, S.J., Scheuer, P.J., 1996. Kulolide: a cytotoxic depsipeptide from a cephalaspidean mollusk, *Philinopsis speciosa*. J. Am. Chem. Soc. 118, 11081−11084. https://doi.org/10.1021/ja9620301.

Salvador, L.A., Biggs, J.S., Paul, V.J., Luesch, H., 2011. Veraguamides A−G, cyclic hexadepsipeptides from a dolastatin 16-producing cyanobacterium *Symploca* cf. *hydnoides* from Guam. J. Nat. Prod. 74, 917−927. https://doi.org/10.1021/np200076t.

Tan, L.T., 2007. Bioactive natural products from marine cyanobacteria for drug discovery. Phytochemistry 68, 954−979. https://doi.org/10.1016/j.phytochem.2007.01.012.

Tan, L.T., 2010. Filamentous tropical marine cyanobacteria: a rich source of natural products for anticancer drug discovery. J. Appl. Phycol. 22, 659−676. https://doi.org/10.1007/s10811-010-9506-x.

Tan, L.T., Phyo, M.Y., 2020. Marine cyanobacteria: a source of lead compounds and their clinically-relevant molecular targets. Molecules 25, 2197. https://doi.org/10.3390/molecules25092197.

Tranter, D., Paatero, A.O., Kawaguchi, S., Kazemi, S., Serrill, J.D., Kellosalo, J., Vogel, W.K., Richter, U., Mattos, D.R., Wan, X., Thornburg, C.C., Oishi, S., McPhail, K.L., Ishmael, J.E., Paavilainen, V.O., 2020. Coibamide A targets Sec61 to prevent biogenesis of secretory and membrane proteins. ACS Chem. Biol. 15, 2125−2136. https://doi.org/10.1021/acschembio.0c00325.

Tripathi, A., Puddick, J., Prinsep, M.R., Lee, P.P., Tan, L.T., 2009. Hantupeptin A, a cytotoxic cyclic depsipeptide from a Singapore collection of *Lyngbya majuscula*. J. Nat. Prod. 72, 29−32. https://doi.org/10.1021/np800448t.

Tripathi, A., Puddick, J., Prinsep, M.R., Lee, P.P.F., Tan, L.T., 2010. Hantupeptins B and C, cytotoxic cyclodepsipeptides from the marine cyanobacterium *Lyngbya majuscula*. Phytochemistry 71, 307−311. https://doi.org/10.1016/j.phytochem.2009.10.006.

Yang, L., Barken, K.B., Skindersoe, M.E., Christensen, A.B., Givskov, M., Tolker-Nielsen, T., 2007. Effects of iron on DNA release and biofilm development by *Pseudomonas aeruginosa*. Microbiology 153, 1318–1328. https://doi.org/10.1099/mic.0.2006/004911-0.